

i. Imaging-based analysis of cell-cell contact dependent migration in *Dictyostelium*

Taihei Fujimori¹, Hidenori Hashimura² and Satoshi Sawai^{2*}

*author correspondence: cssawai@mail.ecc.u-tokyo.ac.jp

¹*Department of Bioengineering, Stanford University, Stanford, CA, USA*

²*Graduate School of Arts and Sciences, The University of Tokyo, Tokyo, Japan*

© 2023 Taihei Fujimori. All Rights Reserved.

ii. Summary/Abstract

Cell-cell interaction mediated by secretive and adhesive signaling molecules forms the basis of the coordinated cell movements (i.e. collective cell migration) observed in developing embryos, regenerating tissues, immune cells and metastatic cancer. Decoding the underlying input/output rules at the single-cell level, however, remains a challenge due to vast complexity in the extracellular environments that support such cellular behaviors. The amoebozoia *Dictyostelium discoideum* uses GPCR-mediated chemotaxis and cell-cell contact signals mediated by adhesion proteins with immunoglobulin-like folds to form a collectively migrating slug. Coordinated migration and repositioning of the cells in this relatively simple morphogenetic system is driven strictly by regulation of actin cytoskeleton by these signaling factors. Its unique position in the eukaryotic tree of life outside metazoa points to basic logics of tissue self-organization that are common across taxa. Here, we describe a method to reconstitute intercellular contact signals and the resulting cell polarization using purified adhesion proteins. In addition, a protocol using a microfluidic chamber is laid out where one can study how the cell-cell contact signal and chemoattractant signals when simultaneously presented are interpreted. Quantitative image analysis for obtaining cell morphology features is also provided. A similar approach should be applicable to study other collectively migrating cells.

iii. Key Words

cell-cell contact, collective cell migration, chemotaxis, microfluidics, protein purification, image analysis

1. Introduction

Coordinated cell movements require cell-cell communication. Its disruption is associated with cancer metastasis and tissue malformation that results from disordered cell movements and migration. There are two modes of communication: 1) diffusive secreted factors that act at a distance and 2) local cell-cell contact signals (or 'juxtacrine' signal) by adhesion molecules and their complex on the cell surface [1, 2]. Diffusive molecule signals are thought to form concentration gradients and control the direction of cell motility by inducing cell attraction or repulsion responses (so called chemotaxis). In metazoans, the lateral line of zebrafish migrates towards self-generated SDF-1 gradient; directed migration of border/polar cell clusters of fruit fly is mediated by EGF gradient [3]. As for the contact signals, the well-known cell-cell contact-dependent inhibition of locomotion in *Xenopus* development is mediated by the adhesion molecule Cadherin [4]. Activated lymphoblasts are known to move as small clusters in an integrin/ICAM-1 dependent manner [5]. Identifying these key factors only solves a part of the problem, since cells likely make use of combinations of these signals to regulate the cytoskeletal and membrane dynamics. *Ex vivo* and *in vitro* assays have the potential to distinguish and clarify the contribution of each signal by allowing one to study cell dynamics in a more defined and controlled environment. In *Xenopus* neural crest cells, for example, observation of locomotion of an *ex vivo* cell cluster has shown that the directional motion of these cell clusters under a reconstituted chemoattractant stimulus requires cell-cell contact dependent inhibition of

locomotion that confers cell polarity [6, 7]. Live-imaging of dorsal marginal zone explants extracted from a *Xenopus* embryo has pointed out the importance of higher Ca^{2+} levels in the leading cells than the following cells for gastrulation [8]. These examples still require some degree of cell-cell contacts and extracellular environments that had already formed *in vivo*, full dissociation of the tissue or removal of embryonic extracts are often detrimental to the coordinated migration indicating that there are still many unknowns in the system. One can alternatively turn to cancer lines with epithelial characteristics, for example, to study how leading cells appear in a cell-culture setup. There one can observe the behavior of cell collectives under controlled geometry by plating cells on patterned adhesion substrates on glass [9]. There is still a large gap between what can be tested at the single-cell level and how one can relate it to the migratory behavior *in vivo*.

Interestingly, a non-metazoan system - the social amoeba *Dictyostelium discoideum* - shows similar collective cell migratory behavior and provides a unique point of analysis that is noteworthy from both cell mechanics and evolutionary perspectives. These cells form relatively simple multicellular bodies by cell aggregation under starved conditions. Owing to this conditional multicellularity and its genetic tractability, the system is amenable to detailed single-cell level live-cell imaging studies. With almost no cell division and cell death in the process, deciphering how directed migration and cell polarity is dictated within the multicellular context directly translates to understanding of the pattern formation dynamics. Numerous imaging-based and molecular biology studies have shown that both chemotaxis toward cAMP and cell-cell adhesion molecules TgrB1 and TgrC1 are involved in the morphogenetic cell movements in the early aggregate [10]. More recently, it was shown that the TgrB1 and TgrC1 acting *in trans* between adjacent cells induce recruitment of the SCAR/WAVE complex to the cell-cell contact site and hence forms the basis of F-actin formation and the resulting head-to-tail cell alignment observed in the multicellular aggregates [11]. This contact-dependent response

can be analyzed at the single-cell level using beads coated with purified TgrC1 [11]. Furthermore, a microfluidic PDMS device with a low ceiling that constrains cells in a pseudo-2D environment [11] is of use to dissect the role of cell-cell contact in cell cluster migration as it makes it easier to extract cell contour and analyze its deformation (Fig. 1a,b). By using the device, it was revealed that follower cells in a cell cluster show enhanced cell polarity with more ballistic motion and prioritize contact-dependent following motion over chemotaxis [11]. In this chapter, detailed experimental setup for Tgr-coated beads and microfluidics as well as image analysis are described. In particular, we provide guides to prevent some of the most frequently encountered troubles with the microfluidics operations. Although the protocol described is designed specifically to *Dictyostelium*, similar experimental/analysis techniques should be applicable to other systems.

2. Materials

2.1. Cell culture media and buffers

1. PS medium (1L): In a cylinder, pour about 800 mL water then mix the following:
10 g special peptone (712072-5, OXOID), 7g yeast extract (712021-5, OXOID), 0.12 g $\text{Na}_2\text{HPO}_4 \cdot 7\text{H}_2\text{O}$ (191441, MP Biomedicals) and 1.4 g KH_2PO_4 (169-04245, Wako) using a magnetic stir bar. Top it up with water to 900 mL and autoclave. Cool the autoclaved media to room temperature. Add the 100 mL supplement solution by passing it through a 0.22 μm filter for sterility and store at 4°C.
2. Supplement solution (100 mL): Dissolve 15 g dextrose (215530, Difco Lab) in 50 mL water, add folic acid (060-01802, Wako) and vitamin B12 (220-00341, Wako) 800 ng/mL and 400 ng/mL respectively. Add 10 mL

Antibiotic-Antimycotic mix (15240062, Invitrogen) to the dextrose solution then add water to the final volume of 100 mL.

3. 10×PBS: Mix 40 g NaCl (192-13925, Wako), 1 g KCl (163-03545, Wako), 1.2 g KH_2PO_4 , 13.4 g $\text{Na}_2\text{HPO}_4 \cdot 7\text{H}_2\text{O}$ in 500 ml water. Autoclave and store at 4°C. Use at 1× concentration.
4. 10×Phosphate Buffer (PB): Add 8.16 g KH_2PO_4 , 10.7 g $\text{Na}_2\text{HPO}_4 \cdot 7\text{H}_2\text{O}$ in 500 mL water. Check that the pH is 6.5. Sterilize by autoclave and store at 4°C. Use at 1× concentration.
5. Developmental Buffer (DB): Mix 25 mL 10×PB, 455 mL water, 10 mL 0.01 M CaCl_2 (039-00475, Wako) and 10 mL 0.1 M Mg_2SO_4 (131-00405, Wako). Check that the pH is 6.5. Sterilize by autoclave and store at 4 °C.
6. DB agar: Add 1 % Bacto Agar (010-08725, Wako) in DB, autoclave or microwave it to dissolve. Pour 4 mL agar in a 6 cm dish. Store at 4 °C.
7. cAMP solution: Dissolve cAMP (A6885, Sigma-Aldrich) in PB at 1 mM as a 1000X stock. Aliquot 15 μL and store at -30°C (up to three freeze-thaw cycles are preferred). To visualize cAMP gradient in the microfluidic device, add f.c. 3 μM fluorescein (231-00092, Wako), 5 $\mu\text{g/mL}$ ATTO425 (AD425-21, ATTO TEC) or 4 $\mu\text{g/mL}$ Alexa594 (A10438, Invitrogen). Dye should be chosen to avoid overlap with the spectrum of the fluorescent protein (GFP, RFP etc) expressed by the cells being analyzed.

2.2. Protein purification and affinity beads

1. Ni²⁺-NTA column His Trap FF crude, 5 mL (17-5286-01, GE). Prepare 20 mM Imidazole/PBS and 500 mM Imidazole/PBS using solutions that come with this kit.
2. Amicon Ultra 15 mL 50K (UFC905008, Millipore)
3. Amicon Ultra 0.5 mL 50K (UFC505008, Millipore)
4. Affinity beads (BS-X9905, Sumitomo Bakelite). Fixation buffer and inactivation buffer come with the kit.
5. Wheat Germ Agglutinin (WGA) (126-02811, Wako)

2.3. Microfluidics equipment

1. Air compressor (2522C-05, Welch)
2. Pressure regulator (MFCS™-FLEX, Fluigent)
3. Flow controller (Flowell, Fluigent)
4. Laptop PC with MAESFLO (Fluigent) software
5. PEEK tubing OD 1/32" ID 0.25 mm (NPK-007, ARAM)
6. Union 1/32" OD to 1/16" OD (P-881, Upchurch Scientific)
7. 1/16" × 0.5 mm ETFE tube (6010-36510, GL Sciences)
8. Silicon tube (94-2001, SANYO)
9. Male luer fitting (VRSP6, ISIS)
10. Female luer fitting (VRF106, ISIS)
11. PDMS (Sylgard 184 Silicone Elastomer kit, Dow Corning)

12. 24 mm × 50 mm No. 1 coverglass (C024501, Matsunami)

3. Methods

3.1. Tgr protein purification

1. Suspend TgrB1^{ext}-His₆/AX4 or TgrC1^{ext}-His₆/AX4 cells in 660 mL PS media at the density of 1×10^6 cells/mL. The cells express His₆-tag-conjugated extracellular domain of TgrB1(from Met1 to Thr802) or TgrC1(from Met1 to Asn851), respectively. These domains were cloned at the downstream of constitutively active actin15 promoter so that these extracellular domains are expressed in the vegetative cells, and secreted to the culture media due to the lack of transmembrane domain. Divide the cell suspension into two 330 mL cultures in a 1L Erlenmeyer flask. Culture for 2 days by shaking at 125 rpm at 22°C. Avoid exposing the culture to room light as it inhibits cell proliferation. Cover the flask with foil if necessary.
2. Cell density should be around 1×10^7 cells/mL after 2-days culture. Spin down the cells at 700 ×g, 4 °C, 3 minutes. Filtrate the supernatant using a 100 mL syringe with a 0.45 µm filter.
3. Allow the secreted Tgr-His₆ proteins to bind to Ni²⁺-NTA affinity column (His Trap FF crude) by passing the filtered supernatant at 1 mL/min. Use of an automated purification system such as the AKTA system is recommended for automation of this step.
4. Wash the column with 20 mM Imidazole/PBS, then elute with 20 mL of 500 mM Imidazole/PBS.

5. Check the molecular weight by performing western blotting against His₆-tag for the input sample and the eluate. The expected molecular weight is around 150 kDa for TgrC1, and 130 kDa for TgrB1 [12].
6. Check the purity by performing coomassie brilliant blue staining for the input sample and the eluate. There may be a light smear originating from the growth medium below 50 kDa which will be removed in the eluate.
7. Reduce the volume of the eluate from 20 mL to 2 mL using a 50kDa-cutoff column (Amicon Ultra 15 mL 50K). To remove imidazole and salt in the sample, dilute it to 15 mL with PB, then concentrate again with the Amicon filter to 2 mL. Repeat it one more time. Concentrate the sample further to 700 μ L. As measured by A280 absorbance, the final yield is typically around 0.1~0.6 mg/mL.

3.2. Coating affinity beads

1. Suspend 2 to 4 mg of dried affinity beads in a 400 μ L fixation buffer.
2. Concentrate 20 μ g Tgr proteins using amicon Ultra tube 0.5 mL 50K to ~20 μ L.
3. Add 20 μ g purified Tgr and WGA with the beads. Facilitate the crosslinking reaction between proteins and beads by mixing on a rotator at 30 rpm at room temperature overnight.
4. Spin down the beads at 16100 $\times g$, 4 $^{\circ}$ C, 1 minute. Remove the buffer, Resuspend in 500 μ L PBS.
5. Repeat step 4 twice.
6. Spin down and remove PBS, add 400 μ L of inactivation buffer. Rotate at room temperature for 1 hour.

7. Spin down and resuspend in 500 μL PBS three times. Spin down and resuspend in 200 μL PBS.

3.3. Observation of the contact-dependent F-actin formation

1. To obtain differentiated cells, spin down 1.87×10^7 Lifeact-RFP/AX4 cells at $700 \times g$, 4°C , 3 minutes. Lifeact is a commonly used small peptide that binds to F-actin. Resuspend in 5 mL DB and spin down again. Resuspend in 5 mL DB then pour the cell suspension on a DB agar. Leave the dish at room temperature for 10 minutes. Aspirate DB and dry the agar surface. Incubate at 22°C for 17~21 hours.
2. Collect multicellular bodies (slugs) in 1xPB using a cell scraper. Dissociate cells by passing the cell suspension through a 23-gage needle back and forth using a 1 mL syringe.
3. Dilute cell suspension to 1×10^5 cells/400 μL 1xPB, then add 3~5 μL Tgr-coated beads.
4. Add cell suspension with the beads to a 24-well glass bottom dish. Leave 30 minutes at room temperature.
5. Start imaging. Around 45% of the cells in contact with the beads should show persistent F-actin formation at the bead-cell contact site and cell elongation.

3.4. Preparation of chemotactic-competent cells by cAMP pulsing

1. Wash cells three times by spinning down and resuspending the cells in PB. Suspend washed cells at the density of 5×10^6 cells/mL in 5 mL PB. Shake the cell suspension in a flask at 125 rpm at 22°C for 1 hour.

2. Add cAMP pulses at 6 minutes intervals at the final concentration of 50 nM for 6 to 8 hours.
3. Centrifuge cells and resuspend in 2.5 mL PB.

3.5. Setting up the perfusion system

1. Assemble the Flowell following manufacturer instructions. For details of Flowell assembly, follow section 3.2 step 1 ~ 6 in ref. [13] with the following modifications. For step 4 and 5 in ref. [13], use 1/32" PEEK tubing instead of 0.5 mm OD PEEK tube and sleeve. For step 6, use the ETFE tube instead of PEEK tubing ((c)~(e) in Fig. 1c in ref. [13]) for all output ports. Skip steps 7 ~ 9.
2. Check if all tubes are connected correctly (Fig. 1c).
3. Connect MFCS-FLEX to Flowell, an air compressor and a laptop computer. Turn on the air compressor, MFCS, and the laptop computer. Make sure all tubes on MFCS are disconnected from Flowell, and the MFCS is placed on a well-leveled table top. Run the MAESFLO software. It takes ~10 minutes for the MFCS to complete pre-heating.
4. Pass PB and cAMP solution through a 0.22 μ m filter.
5. Remove debris in three reservoir tubes by pipetting and discarding 1mL water twice.
6. Fill the three reservoir tubes each with 1 mL 100% EtOH. Attach the reservoir tubes to Flowell, perfuse EtOH in the tubings to wash inside the tubes. Similarly, perfuse the tubings with 1mL water followed by 1 mL PB.
7. Add 1 mL PB in the reservoir tube #2. Add 1 mL PB containing 1 μ M cAMP in the reservoir tube #1 and #3. Attach the reservoir tubes to Flowell (Fig. 1c).

3.6. Debubbling the PDMS device and cell loading

1. Cure a microfluidic PDMS device following a standard protocol [14, 15]. Note that the device mold consists of two layers of SU-8 spin-coated on a silicon wafer (Fig. 1b). Use a 1.5 mm biopsy punch to make a hole where the ETFE tubes are attached. Use a 24 mm × 50 mm No. 1 coverglass to bond the PDMS device.
2. Connect an ETFE tube attached with a female luer fitting through silicon tube to the outlet of the microfluidic PDMS device. Attach a 5 mL syringe filled with 5 mL filtered PB. Perfuse PB into the device by pushing the syringe until droplets come out from other inlets/outlets (Fig. 2a).
3. Connect an ETFE tube with a female luer fitting to the cell inlet/outlet. Plug the inlet #1~#3 with plastic sticks (any acrylic plastic rod works). Set the device on a stage adapter and tape it (Fig. 2b). Place the device on the microscope. Put some paper towels so as to prevent the microscope from getting wetted by perfused reagents (Fig. 2b).
4. To plug the cell inlet/outlet, first fill the inside of male luer fitting with PB and connect it to the female luer fittings. Fuse the droplets on the luer fittings not to introduce bubbles (Fig. 2c).
5. Find the cell loading channels (5 μ m height layer) under the microscope (Fig. 1b; red layer, Fig. 2d(i); orange rectangle). Perfuse PB from the outlet with a 5 mL syringe. Bubbles in the cell loading channels should disappear owing to gas permeability of the PDMS (Fig. 2d(i)).
6. Check the inlet #1~#3 under the microscope. In case bubbles remain, perfuse PB until all bubbles disappear (Fig. 2d(ii)).

7. Remove male luer fittings on the cell inlet/outlet.
8. Attach a 1 mL syringe filled with cell suspension to the cell inlet. Make sure that there are no bubbles when the syringe is attached (Fig. 3a), and an unplugged cell outlet is on a paper towel to absorb the drain (Fig. 3b(i)). Load cell suspension. It is recommended that one observe cell loading to the cell loading channels under the microscope (Fig. 3b(ii)).
9. Remove the syringe with the cell from the cell inlet. Plug the cell inlet/outlet with male luer fittings.
10. Move the device on a flat surface on the microscope stage (Fig. 3c(i)).
11. Make droplets on the inlet #1 ~ #3 by pushing the 5 mL syringe at the outlet.
12. Remove the 5 mL syringe from the outlet.
13. Connect the Flowell tubes from cAMP reservoirs to the inlet #1 and #3, and connect Flowell tubes from PB reservoir to the inlet #2 (Fig. 3c(ii)). Make sure that there are no bubbles when the tubes are connected.
14. Place the device on the stage adapter again. Tape the device and tubes so as to prevent them from being disturbed during imaging (Fig. 3d).

3.7. Perfusion and live-cell imaging

1. Perfuse the buffer through Flowell at 20~30 $\mu\text{L}/\text{min}$ for 5 minutes and wait for the flow to stabilize.
2. Adjust the flow speed around 5-6 $\mu\text{L}/\text{min}$ for PB flow and ~2 $\mu\text{L}/\text{min}$ for cAMP flow. At this point, cells have not been exposed to cAMP in the microfluidics chamber.

3. Make one of the cAMP flows to 5~6 $\mu\text{L}/\text{min}$ to create cAMP gradient in the cell loading channels (Fig. 4a).
4. Set the focus to the cells of interest. Start live imaging.
5. After 1 minute, run a script for the automated fluidic control system operation for the gradient reversal (See note for the sample script). Gradient reversal is completed in 1 minute (Fig. 4b,c). For the estimate of the cAMP concentration, take images after filling/removing fluorescent molecules from the entire channel as reference points for 1 and 0 μM cAMP respectively (the detail of calculation is described in [13]). Solitary migrating cells form lateral pseudopods and turn towards the reversed gradient in 4 minutes (Fig. 4d,e).

3.8. Image analysis

1. Any of the established cell migration analysis algorithms should be applicable for the data obtained. Here we describe a typical analysis to quantify the local velocity, curvature and fluorescent intensity on segmented cell boundaries. MATLAB codes to perform this analysis are available at the author's github repository (<https://github.com/fjmr/BoundaryTrack>). This is GUI-based automated boundary segmentation, tracking and quantification.
2. Preprocessing is required to obtain the binarized fluorescent images. For fluorescent images with high contrast, Otsu binarization performed on ImageJ (<https://imagej.nih.gov/ij/>) works well. If the signal-to-noise ratios in fluorescence images are low, we recommend taking a machine-learning based approach using the Fiji plugin Trainable Weka segmentation [16]. The plugin supports a convenient pipeline from annotating data, training the neural network and generating the final segmentation (Fig. 5a).

3. The detail of the algorithm of the segmentation and tracking, quantification is described in the repository noted above. In brief, the algorithm detects and segments the contour of the binarized image and then determines the mapping of successive images by minimizing sum of squared distances of corresponding segments (Fig. 5b). A similar analysis can be done using QuimP [17].
4. Heatmap is helpful to visualize the dynamics of local velocity, curvature and fluorescent intensity change (Fig. 5c). Representative response is 1) the retraction of existing leading edge as evident in the decrease of F-actin intensity and velocity (purple rectangles; Fig. 5c) and 2) the formation of lateral leading edge as evident in the increase of F-actin intensity, velocity and curvature (purple circles; Fig. 5c).

4. Notes

4.1. Tgr purification

1. High cell density results in decreased yield due to cell death.
2. Covering the flask with foil is important when the culture flask is shaken under room light. Otherwise, cells don't grow.
3. For coating purified proteins on beads, any commercially available beads with functional groups on their surface for covalent bond formation to primary amino groups of the purified protein should work. The diameter of the beads should be smaller than the cell size to mimic cell-cell contact (around 5 μm is preferred). Although we have not tested, the 2.8 μm diameter Dynabeads™ M-270

Carboxylic Acid (14306D, Invitrogen) follows the same reaction and should work for this purpose.

4.2. Microfluidics

1. The optimal flow rate that supports formation of a preferred gradient in the cell loading channels can differ for every new PDMS device made even if they are of the same design. It is recommended to check the gradient beforehand.
2. The male luer fittings and syringes should be removed gently. Negative pressure in the cell loading channels could squash the cells.
3. Using a smaller coverslip (e.g. 24 mm×50 mm) makes the device harder to bend, which helps prevent the device from drifting in the vertical axis and losing the focus.
4. Connecting/disconnecting tubes to the device on a stage adapter can easily introduce enough strain to crack the coverslip. Work with the device on a flat surface to avoid this.
5. Sample code for gradient reversal. Save this code as 'grad1.au3'. Modify the values in the Pressure function to achieve a reversed gradient.

```
#include <Group.au3>
```

```
Init()
```

```
=====
```

```
; The Script must start with #include <Group.au3>
```

```
; directly followed by Init() sequence
```

```
; Do not change this initialization
```

```

; Do not change the file Group.au3

; The user scripts start after this commentary sequence

; Case insensitive

;=====

Pressure(6.8,6,0,4)

End() ;You MUST end the script with this order!

```

5. Acknowledgements

This work was supported by Japan Society for the Promotion of Science (JSPS) KAKENHI Grant 19H05801 and Japan Science and Technology Agency (JST) CREST JPMJCR1923 (to S.S.). T.F. was supported by JSPS Fellowship Grant JP17J08690. H.H. was supported by MEXT KAKENHI Grant 20J00751 and 21K15081.

6. References

1. Mayor R, Etienne-Manneville S (2016) The front and rear of collective cell migration. *Nature Reviews Molecular Cell Biology* 17:97–109
2. Mishra AK, Campanale JP, Mondo JA, Montell DJ (2019) Cell interactions in collective cell migration. *Development* 146.: <https://doi.org/10.1242/dev.172056>
3. Scarpa E, Mayor R (2016) Collective cell migration in development. *J Cell Biol* 212:143–155
4. Carmona-Fontaine C, Matthews HK, Kuriyama S, et al (2008) Contact inhibition of locomotion in vivo controls neural crest directional migration. *Nature* 456:957–961
5. Malet-Engra G, Yu W, Oldani A, et al (2015) Collective cell motility promotes chemotactic prowess and resistance to chemorepulsion. *Curr Biol* 25:242–250
6. Theveneau E, Marchant L, Kuriyama S, et al (2010) Collective chemotaxis requires contact-dependent cell polarity. *Dev Cell* 19:39–53

7. Carmona-Fontaine C, Theveneau E, Tzekou A, et al (2011) Complement fragment C3a controls mutual cell attraction during collective cell migration. *Dev Cell* 21:1026–1037
8. Hayashi K, Yamamoto TS, Ueno N (2018) Intracellular calcium signal at the leading edge regulates mesodermal sheet migration during *Xenopus* gastrulation. *Sci Rep* 8:2433
9. Coordination of cell migration mediated by site-dependent cell–cell contact. In: PNAS. <https://www.pnas.org/content/pnas/115/42/10678>. Accessed 31 Mar 2022
10. Dynes JL, Clark AM, Shaulsky G, et al (1994) LagC is required for cell-cell interactions that are essential for cell-type differentiation in *Dictyostelium*. *Genes Dev* 8:948–958
11. Fujimori T, Nakajima A, Shimada N, Sawai S (2019) Tissue self-organization based on collective cell migration by contact activation of locomotion and chemotaxis. *Proc Natl Acad Sci U S A* 116:4291–4296
12. Chen G, Wang J, Xu X, et al (2013) TgrC1 mediates cell–cell adhesion by interacting with TgrB1 via mutual IPT/TIG domains during development of *Dictyostelium discoideum*. *Biochem J* 452:259–269
13. Nakajima A, Sawai S (2016) Dissecting Spatial and Temporal Sensing in *Dictyostelium* Chemotaxis Using a Wave Gradient Generator. *Methods Mol Biol* 1407:107–122
14. Fukujin F, Nakajima A, Shimada N, Sawai S (2016) Self-organization of chemoattractant waves in *Dictyostelium* depends on F-actin and cell–substrate adhesion. *J R Soc Interface* 13:20160233
15. Nakajima A, Ishida M, Fujimori T, et al (2016) The microfluidic lighthouse: an omnidirectional gradient generator. *Lab Chip* 16:4382–4394
16. Arganda-Carreras I, Kaynig V, Rueden C, et al (2017) Trainable Weka Segmentation: a machine learning tool for microscopy pixel classification. *Bioinformatics* 33:2424–2426
17. Baniukiewicz P, Collier S, Bretschneider T (2018) QuimP: analyzing transmembrane signalling in highly deformable cells. *Bioinformatics* 34:2695–2697

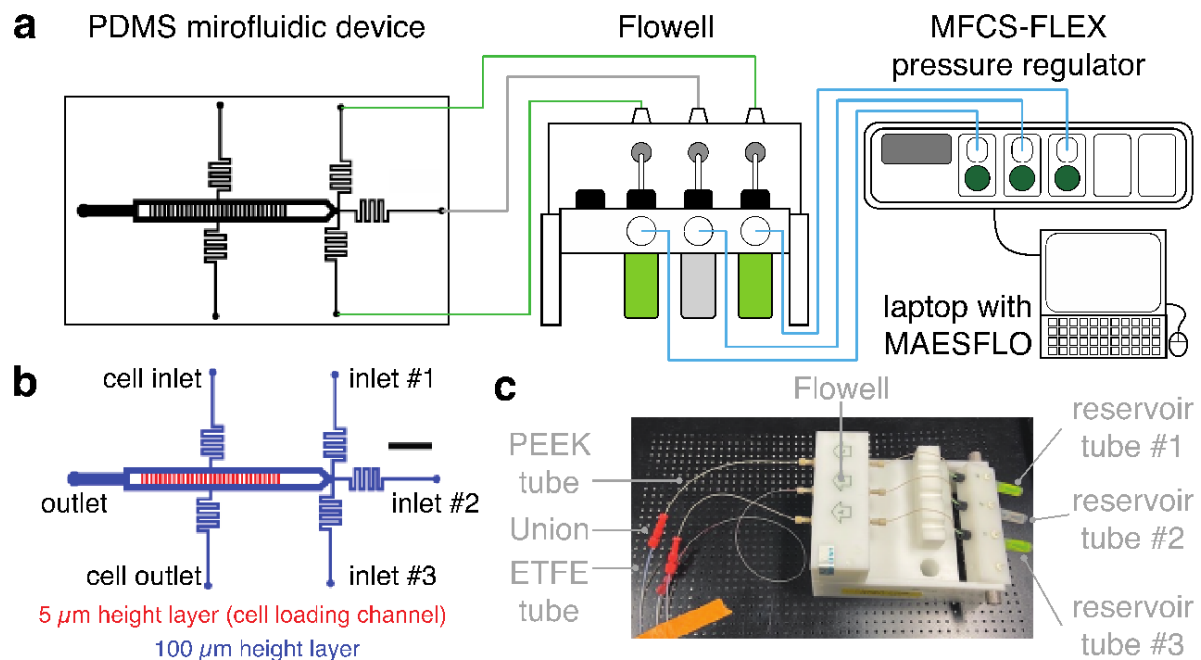


Fig. 1 The overview of the fluidics system for gradient reversal. (a) A schematic of the entire fluidics system. (b) The microfluidic device for gradient reversal. Scale bar, 2 mm. (c) Assembly of Flowell.

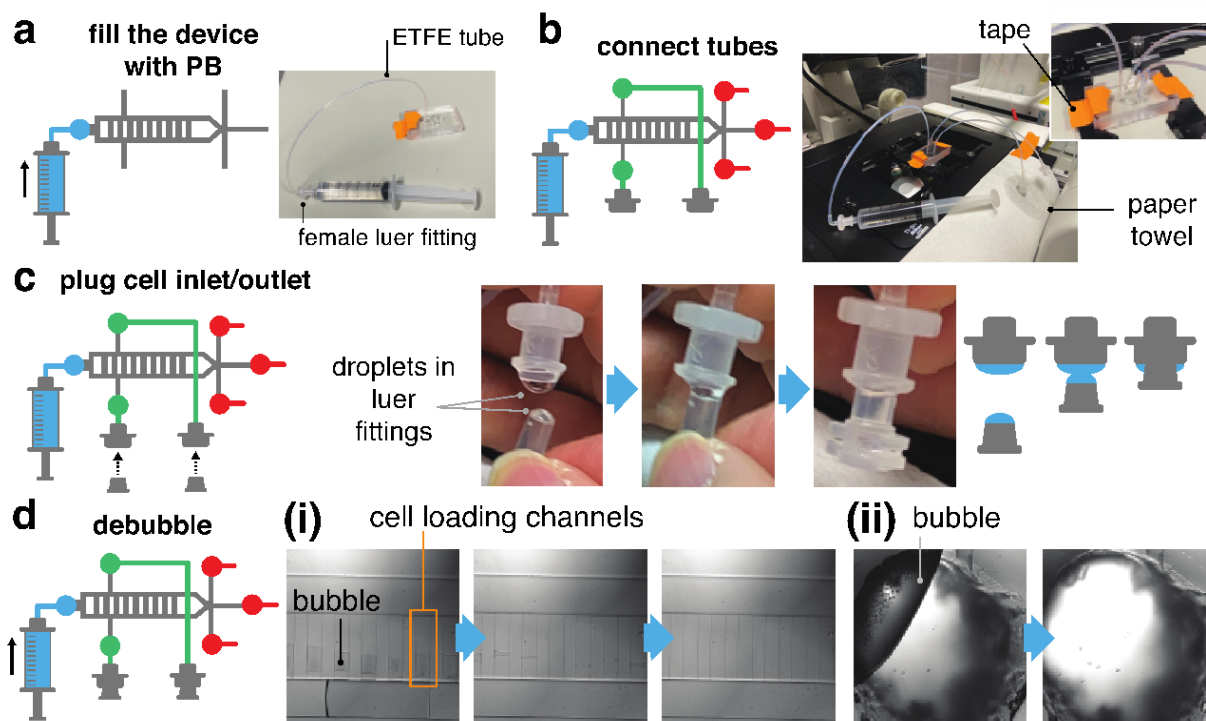


Fig. 2 Debubbling the PDMS microfluidic device. (a) An ETFE tube attached to a syringe (blue) is connected to the outlet to fill the device with PB. (b) Inlets #1~#3 are sealed with small plastic rods (red). ETFE tubes are attached to the cell inlet/outlet (green). Secure the device on the stage adapter. Use of a masking tape is practical. Paper towels are placed to absorb the drain. (c) Connect luer fittings without introducing bubbles by fusing water interfaces on the luer fittings. (d) Debubble by perfusing PB. i: Bubbles in the 5 μm height cell loading channels appear as grayish areas, which were removed by perfusing PB. ii: Bubbles at the inlets and outlets should also be removed by perfusing PB.

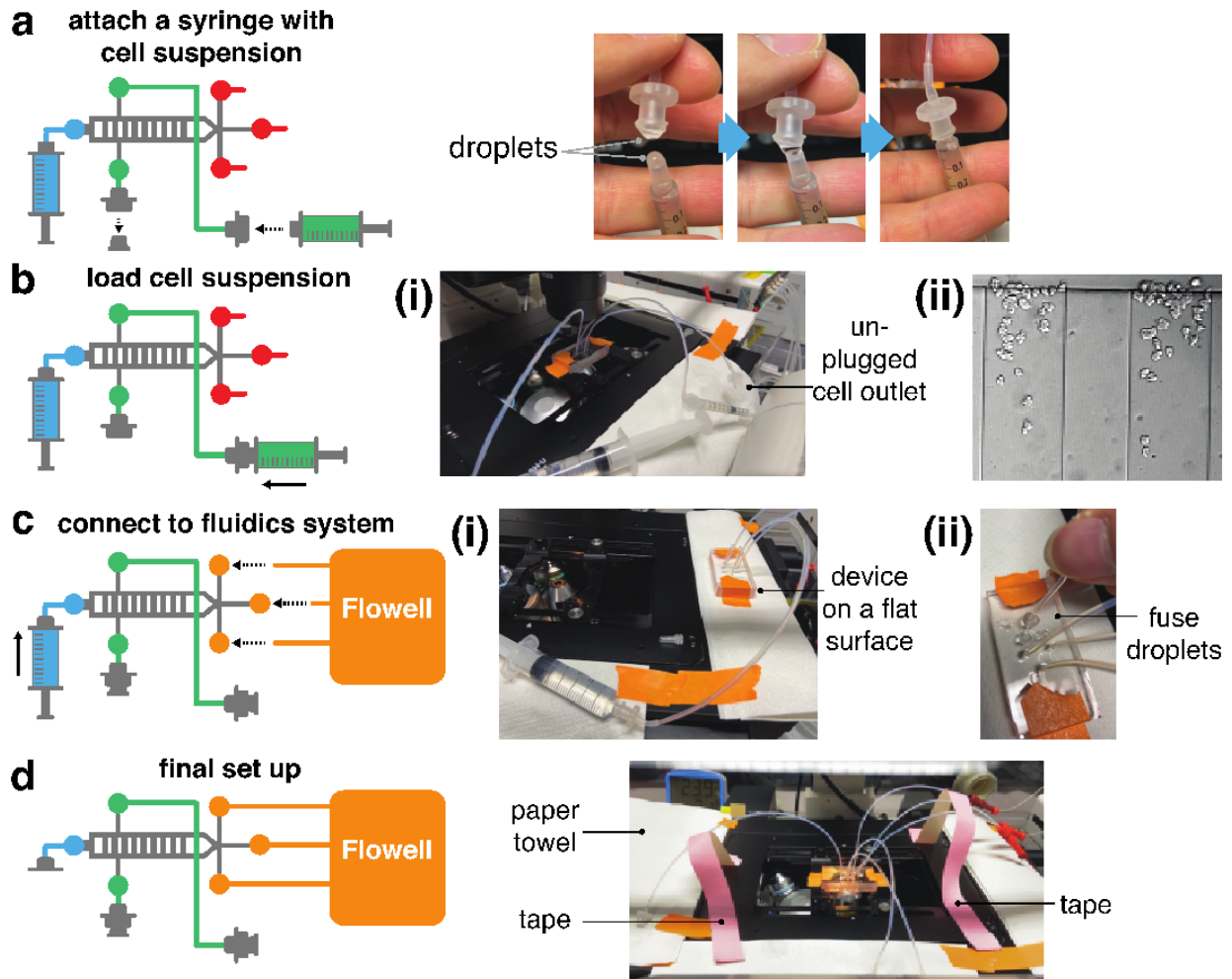


Fig. 3 Cell loading and the staging setup. (a) Connect a syringe to the female luer fitting at the cell inlet without introducing bubbles by fusing water interfaces prior to connecting the joints. (b) Load cells by perfusing cell suspension. i: Cell outlet should be unplugged, and the drain of cell suspension is absorbed by a paper towel. ii: cells are loaded in the cell loading channels (5 μm height layer in Fig. 1b). (c) Connecting the device to the fluidics system. i: The device should be moved from the stage adapter to a flat surface. ii: Connect tubes to the device by fusing water droplets on each side. (d) The completed setup on a microscope stage ready for the perfusion experiment.

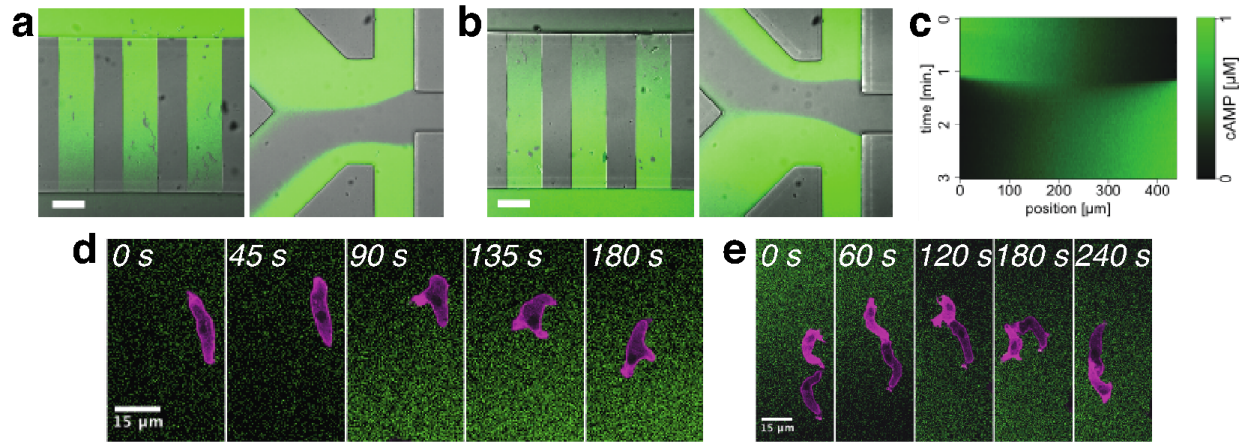


Fig. 4 Gradient reversal experiment. Green: fluorescein in the cAMP solution. (a) Forward gradient. (b) Reverse gradient. (c) The cAMP concentration profile during the gradient reversal estimated from the fluorescence intensity of fluorescein. (d,e) Snapshots from representative time series data. (d) Solitary cell, (e) 2-cell cluster. Magenta: Lifeact-RFP, Green: fluorescein. Scales in (a) and (b) are 100 μm .

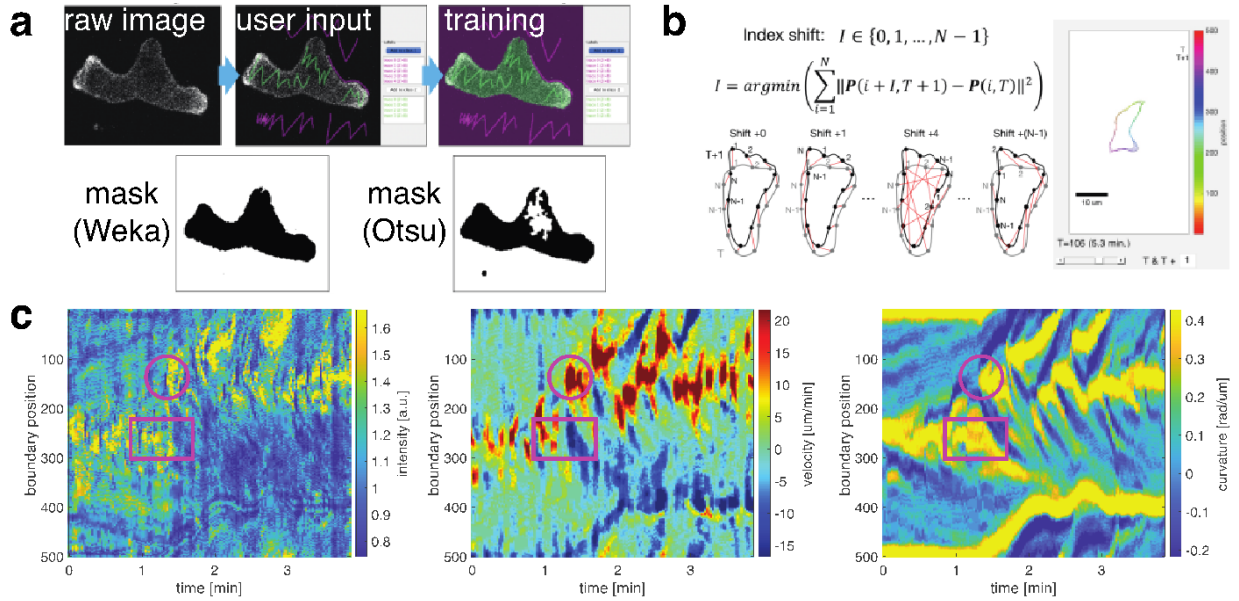


Fig. 5 Image analysis of the cell boundary dynamics. (a) The workflow of trainable Weka segmentation. (b) Algorithm for mapping boundary segments from successive images. Images from the author's github repository (<https://github.com/fjmrt/BoundaryTrack>). (c) Representative data obtained after automated segmentation and calculation of the cell boundary dynamics. Purple rectangles highlight leading edge retraction (note the decrease of F-actin intensity and velocity). Purple circles highlight leading edge formation (note the increase of F-actin intensity, velocity and curvature). Reversal of the cAMP gradient started at time = 54 sec.